Microchimica Acta
https://doi.org/10.1007/s00604-018-3076-z

ORIGINAL PAPER

# Photoelectrochemical determination of the activity of protein kinase A by using g-$C_3N_4$ and CdS quantum dots

Chengji Sui[1] · Fei Liu[2] · Lihua Tang[3] · Xue Li[1] · Yunlei Zhou[1] · Huanshun Yin[1] · Shiyun Ai[1]

Received: 18 July 2018 / Accepted: 28 October 2018


## Abstract

A sensitive and selective photoelectrochemical (PEC) method is described for the detection of protein kinase A (PKA) activity based on the use of graphite-like carbon nitride (g-$C_3N_4$) and the CdS quantum dots (QDs). Firstly, a complex was synthesized from g-$C_3N_4$ and gold nanoparticles (AuNPs). It was employed as both the PEC-active material and as a support for immobilization of peptides. The latter were assembled on an ITO electrode modified with g-$C_3N_4$-AuNPs and subsequently phosphorylated by PKA in the presence of adenosine 5′-[γ-thio]triphosphate (ATP-S). Finally, CdS quantum dots (QDs) were introduced on the ITO in order to increase the PEC response of g-$C_3N_4$ based on the Cd-S binding between the QDs and thiol groups. Under the optimal conditions and a typical working voltage of −0.3 V, the method has a dynamic range that extends from 0.05 to 50 unit·$mL^{-1}$, with a 0.017 unit·$mL^{-1}$ lower detection limit. The method was successfully applied to the quantification of the inhibitory effect of ellagic acid on the activity of PKA, and to monitor enzyme activity in cell lysates.

**Keywords** Protein phosphorylation detection · Graphite-like carbon nitride · Gold nanoparticles · Peptide · Inhibitor screening · Breast tissue · Serum · Signal amplification · Ellagic acid · Specificity

## Introduction

Protein phosphorylation is a kind of crucial post-translational modification, which play critical roles in many biological processes, including cell growth, hormone secretion, gene expression, cell signal communication, metabolism, cell differentiation, and apoptosis [1]. It is well known that protein phosphorylation can be catalyzed by protein kinase, which can transfer phosphate groups from adenosine-triphosphate (ATP) to serine, threonine and tyrosine residues in peptides and proteins. Aberrant protein-phosphorylation states and abnormal expression of kinase activity can lead to many human diseases, including Alzheimer's disease [2], cancer [3] and cardiovascular [4]. Thus, it was of great significance to establish sensitive and selective method for protein kinase activity assay.

Up to now, many methods have been developed for protein kinase activity assay, including radioassay, colorimetry, mass spectrometry, fluorescence, surface plasmon resonance (SPR), raman spectroscopic assay, electrochemical, and photoelectrochemical (PEC) method [5–7], etc. Although these methods can achieve the detection of protein kinase activity, most of them suffer from many shortcomings. For examples, radioactive materials are required in radioassay, which is harmful to the health of the operator. The detection sensitivity of colorimetry needs to be further improved. Mass spectrometry, SPR and raman spectrometry require exquisite and expensive apparatus, sophisticated operation process and skilled operator [8]. Therefore, it is very important to find a fast, sensitive, inexpensive method for protein kinase activity assay. Among the reported methods, the PEC technique, referring to the photocurrent/photopotential change, can be aroused by the biological interactions between various recognition reagents and their corresponding target analytes [9]. Because PEC technique has the superiority of simple and

**Electronic supplementary material** The online version of this article (https://doi.org/10.1007/s00604-018-3076-z) contains supplementary material, which is available to authorized users.

✉ Yunlei Zhou
zhyl@sdau.edu.cn

[1] College of Chemistry and Material Science, Shandong Agricultural University, 271018 Taian, Shandong, People's Republic of China

[2] The Tumor Center of Taian City Central Hospital, Taian, Shandong 271000, People's Republic of China

[3] The Blood Transfusion Division of Taian City Central Hospital, Taian, Shandong 271000, People's Republic of China

Published online: 10 November 2018

inexpensive instrument, low background signal, and high detection sensitivity, it has been proved to be a corking tool for kinase activity detection. So, we chose PEC assay as desired detection method of protein kinase activity.

As we all know, photoactive material is one of the dominant factors for the performance of PEC technique. Up to now, there are many materials have been employed in PEC. For instances, Gao et al. used carbon quantum dot-sensitized $TiO_2$ as photoactive material to achieve the ultrasensitive detection of thrombin [10]. Zhang et al. made a PEC DNAzyme method based ZnO nanoflower to achieve the sensitive detection of $Pb^{2+}$ [11]. Song et al. reported a simple and sensitive PEC method for glucose based on $MoS_2$ ultrathin nanosheets [12]. Moreover, $Bi_2S_3$, BiOI, CuO-$CuWO_4$ and $BiVO_4$-$TiO_2$ have been employed to develop PEC methods in our group [13–16]. Though these materials show great potential in PEC assay there are several disadvantages. On the one hand, some materials (such as $TiO_2$ and ZnO) have the wide band gap, which makes them only absorbs UV light. It can damage some biomolecules to affect the performance of the method [17]. On the other hand, most semiconductor materials contain metals, which may be harmful to environment and human health. In order to overcome these disadvantages, narrow-band gap metal-free material is necessary. Graphite-like carbon nitride (g-$C_3N_4$) has attracted great interest because of its advantages of easy preparation, biocompatibility, high physicochemical stability, metal-free, visible-light response [18]. So far, g-$C_3N_4$ has been widely applied in various fields, such as catalysis, energy storage, photoelectronic devices, optical sensors, and electrochemical sensor [19]. Thus, in our work, g-$C_3N_4$ is chosen as desired photoactive material to construct PEC method for protein kinase A (PKA) activity assay. To achieve sensitive detection, g-$C_3N_4$-AuNPs complex was firstly fabricated, which was used as both photoactive material and the immobilization matrix for peptide. Then, adenosine 5′-[γ-thio]triphosphate (ATP-S) was employed as phosphate group donor and CdS quantum dots (QDs) recognition reagent, where CdS QDs was used as signal amplification unit. Based on the advantages of high detection sensitivity and specificity, PKA activity was successfully detected and the applicability of the PEC method was also investigated. This PEC method also provides a universal platform for other kinases activity assay and screening of inhibitors.

## Experimental

### Reagents and apparatus

Protein kinase A (PKA), mitogen-activated protein kinase (MAPK), Casein Kinase 1 (CK1), Casein Kinase 1 (CK2) were purchased from NEB (USA, https://www.neb.com). PKA kinase activity assay kit was offered by Abcam (https://www.abcam.com). ATP-S was purchased from Sigma-Aldrich Chemical Co. (USA, http://www.sigmaaldrich.com). Tris(hydroxymethyl)aminomethane (Tris), tris(2-carboxyethyl)phosphine hydrochloride (TCEP), thioglycolic acid (TGA), $HAuCl_4$, $CdCl_2$, dithiothreitol (DTT), and ascorbic acid (AA) were supplied by Aladdin (Shanghai, China, https://www.aladdin-e.com). The substrate peptide with sequence of CRRLRRASLG was provided by Sangon Biotech Co., Ltd. (Shanghai, China, https://www.sangon.com). ITO conductive glass (ITO, coating 180 ± 25 nm, sheet resistance <15 Ω/$cm^2$) slices were purchased from Zhuhai Kaivo Electronic Components Co., Ltd. (Zhuhai, China, http://www.zh-kv.com). All other reagents were analytically purity graded and used as received without further purification.

The buffers used in this work are shown below. Peptide immobilization buffer, 20 mM Tris-HCl, 2.0 mM EDTA, 2.0 mM TCEP, 2.0 mM NaCl (pH 7.4). PKA reaction buffer, 0.1 mM EDTA, 0.1 mM DTT, 80 mM ATP-S, 50 mM Tris-HCl, 10 mM $MgCl_2$ (pH 7.4). Washing buffer, 10 mM Tris-HCl (pH 7.4). PEC detection buffer, 100 mM Tris-HCl, 100 mM AA (pH 7.4). Electrochemical impedance spectroscopy (EIS) detection buffer, 5 mM $K_3[Fe(CN)_6]$, 5 mM $K_4[Fe(CN)_6]$, 0.1 M KCl (pH 7.4). Transmission electron microscope (TEM) images were taken with a Tecnai G2 F20 instrument (USA). The photocurrent was recorded on a CHI832A electrochemical workstation (CHI Instruments, Austin, USA). EIS was performed on a CHI660C electrochemical workstation (CHI Instruments, Austin, USA).

### Synthesis of g-$C_3N_4$ and g-$C_3N_4$-AuNPs

The g-$C_3N_4$ was prepared by a typical gradient heating method [20]. Typically, 6.0 g dicyandiamide was put into a tube furnace at 220 °C for 2 h. The ramping rate was 5 °C $min^{-1}$. Then, the temperature was increased to 550 °C for 4 h with ramping rate of 5 °C $min^{-1}$. The sample was cooled naturally to room temperature. Afterwards, the solid was washed with ethanol and deionized water three times. Finally, the prepared g-$C_3N_4$ was dried under vacuum at 60 °C for 6 h.

Next, the g-$C_3N_4$ dispersion solution was prepared by adding 20 mg g-$C_3N_4$ into 10 mL redistilled deionized water during ultrasonic treatment for 30 mins. Then, in the ice bath, the dispersion solution was treated with probe sonicator for 30 min with 300 times of 3 s with an interval of 3 s. Finally, the precipitate was collected with centrifugation at 13800 g for 30 min and dried at 60 °C for 6 h.

g-$C_3N_4$-AuNPs complex were prepared according to the previously reported method [21]. Firstly, 10 μL of 10 mM $HAuCl_4$ was added into the g-$C_3N_4$ dispersion solution under stirring. Next, the solution was sonicated for 10 min and intensely stirred for 30 min at room temperature. This process was repeated for

three times. Then, 25 μL $NaBH_4$ prepared newly was added quickly into the solution, followed by violently stirring for 20 min. Finally, 10 μL of 10 mM sodium citrate was added dropwise into the above suspension and stirred for 30 min. After sufficient reaction, the sample was washed with double-distilled water for three times. The prepared sample was vacuum dried at 60 °C and ground for future use.

## Synthesis of CdS QDs

The CdS QDs was synthesized according to previous reports with minor modification [22]. Firstly, 0.0917 g of solid $CdCl_2$ was added into a round bottom containing 50 mL double distilled water. Then, 250 μL TGA was mixed with the above solution. Next, the pH of the solution was adjusted to 11 with 1.0 M NaOH. The entire experimental procedure was carried out under nitrogen flow. Subsequently, 5.0 mL of 0.1 M $Na_2S$ solution was added dropwise into the round bottom flask with vigorous stirring to obtain a TGA-coated water-soluble CdS QDs. Finally, the mixed solution was refluxed for 4 h under a nitrogen atmosphere. The prepared material was kept at 4 °C for future use.

## Electrode fabrication

The ITO conductive glasses were used as the working electrode, which were cut into 5 × 1 $cm^2$ pieces. Then, the ITO conductive glasses were cleaned by acetone, NaOH solution (1 M, in ethanol and distilled water with *v*/v = 1:1) and distilled deionized water with sonication for 15 min, respectively. Finally, the ITO conductive glasses were washed thoroughly with double distilled water and dried in air. 2 mg of g-$C_3N_4$-AuNPs powder was dispersed ultrasonically in 1 mL of double distilled deionized water, and then 40 μL of the suspension was dropped onto a piece of ITO electrode. The electrode was dried under irradiation of infrared light and named g-$C_3N_4$-AuNP/ITO. For peptide self-assembly, 20 μL of peptide immobilization buffer containing 1.0 μM peptide was dripped on the electrode surface and incubated for 12 h in a humid environment at room temperature. The electrode was then rinsed with washing buffer for three times and the prepared electrode was noted as Peptide/g-$C_3N_4$-AuNP/ITO. Subsequently, 40 μL of 2 mM TGA was dropped on Peptide/g-$C_3N_4$-AuNP/ITO electrode surface and incubated for 1 h in a humid chamber at ambient temperature. After that, the electrode was rinsed with washing buffer for three times to remove the unimmobilized TGA. Then, 40 μL PKA reaction buffer containing different concentration of PKA was dropped on electrode surface and incubated for 40 min in a humid chamber at ambient temperature. The prepared electrode was rinsed with washing buffer for three times and labeled as P-peptide/g-$C_3N_4$-AuNP/ITO. Afterward, 40 μL of CdS QDs was dropped onto the P-peptide/g-$C_3N_4$-AuNP/ITO electrode for 12 h in a humid chamber at ambient temperature. The fabricated electrode (named as CdS/P-peptide/g-$C_3N_4$-AuNP/ITO) was rinsed for three times with washing buffer.

## PEC detection

In this experiment, a three-electrode system was used. The ITO electrode modified with a certain concentration of g-$C_3N_4$-AuNPs composite material was used as the working electrode, and the saturated calomel electrode (SCE) was used as the reference electrode, Pt wire was used as the auxiliary electrode to form a three-electrode system, the three electrodes were placed in the PEC detection buffer to generate photocurrent under illumination conditions, which was completed on the CHI832A electrochemical workstation with visible light. A 500 W Xe lamp was used as the irradiation source. and the

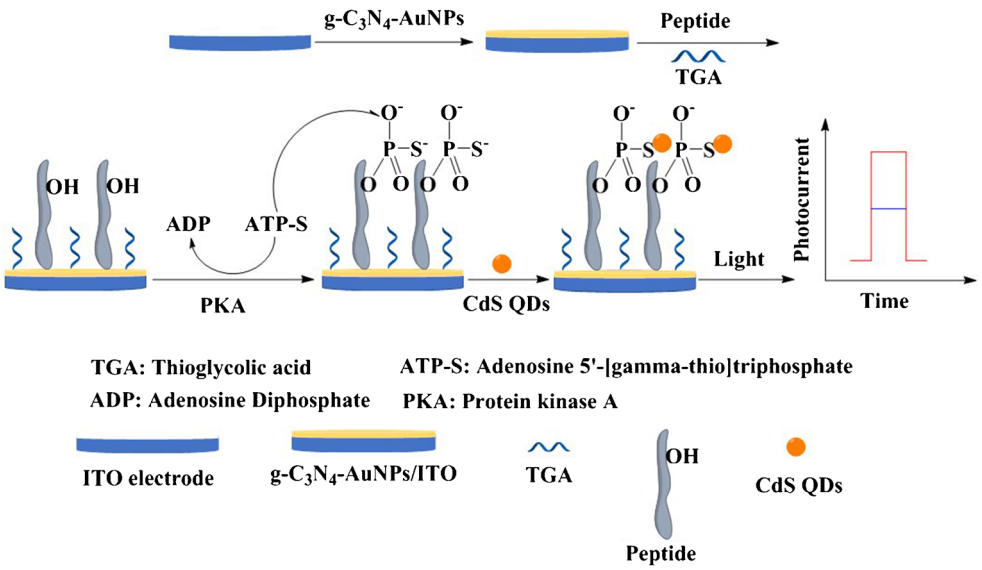


**Scheme 1** Schematic illustration of the fabrication process of the electrode and PEC strategy for PKA activity assay

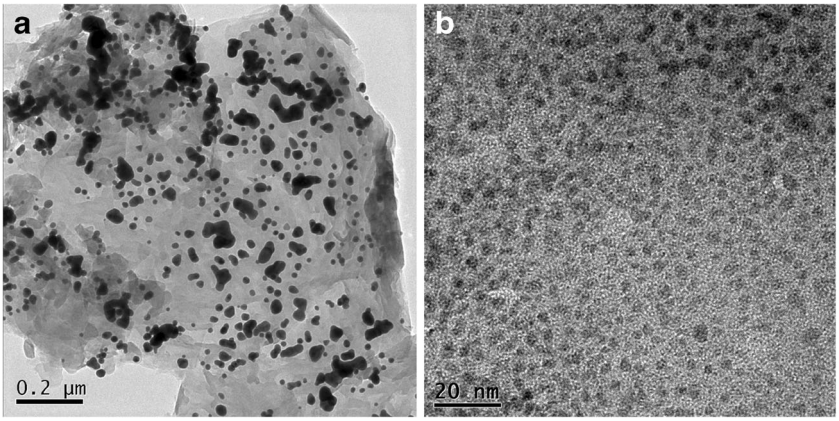


**Fig. 1** TEM image of g-$C_3N_4$-AuNPs (**a**) and CdS QDs (**b**)

detection buffer was deaerated by nitrogen for 30 mins before use, the original potential was −0.3 V for detection.

## Results and discussions

### Detection strategy

In this work, we investigated a novel signal "on" PEC method for PKA activity assay based on g-$C_3N_4$-AuNPs complex and CdS QDs, where g-$C_3N_4$-AuNPs were used as photoactivity substances and peptide immobilization matrix, and CdS QDs was employed as signal amplification unit. As seen in Scheme 1, g-$C_3N_4$-AuNPs is firstly coated on the bare ITO electrode surface through physical adsorption, where the g-$C_3N_4$-AuNPs is not only as photoactivity substance, but also as a linker for the substrate peptide. Based on the reaction between AuNPs and peptide, the substrate peptide is attached on the electrode surface. Subsequently, TGA is introduced as sealing agent to prevent AuNPs on the surface of the electrode to react with other substances. Then the serine residue in the sequence of peptide can be recognized and phosphorylated by PKA in the presence of ATP-S, where one phosphate group with SH is transferred from ATP-S to serine residue. Finally, CdS QDs is introduced to the electrode surface by the Cd-S binding interaction between CdS QDs and phosphorylated serine residue. CdS QDs can accelerate the spatial charge separation, thus preventing the electron–hole recombination, thereby increasing the photocurrent response.

### Characterization of g-$C_3N_4$-AuNPs and CdS QDs

The prepared g-$C_3N_4$-AuNPs was characterized by TEM. As seen in Fig. 1a, lots of black dots are uniformly decorated on the g-$C_3N_4$ surface, indicating that the synthesized AuNPs are tightly anchored on the g-$C_3N_4$ surface. Thus, g-$C_3N_4$-AuNPs complex was prepared successfully. The prepared CdS QDs was also characterized by TEM (Fig. 1b). These CdS QDs are monodispersed with the average diameter about 3–5 nm.

### Detection feasibility assay

To investigate the detection feasibility of the PEC method for PKA detection, the photocurrent density of ITO electrode with different modification process were compared in 0.1 M phosphate buffer containing 0.1 M AA (pH 7.4) under visible light irradiation. As shown in Fig. 2, g-$C_3N_4$/ITO (curve a) presents a well-defined PEC response, indicating that the photoactivity of g-$C_3N_4$. Then when g-$C_3N_4$ is modified with AuNPs, the electrode of g-$C_3N_4$-AuNP/ITO (curve b) showed strong PEC response. It can be attributed to the AuNPs, which facilitate the electron transfer and increase the electrode surface. However, the photocurrent density decreases when the peptide is immobilized on electrode surface (curve c). It can be ascribed to the hindrance effect of peptide, which decreases the transfer activity of electron donor and increases the probability of the recombination of photogenerated electron and hole of g-$C_3N_4$. Then, the photocurrent density further decreases after the serine residue of the peptide is phosphorylated under the catalytic effect of PKA (curve d). With phosphorylation, the negative charge on the peptide increases, which can greatly repel the diffusion of the negative electron donor of AA due to

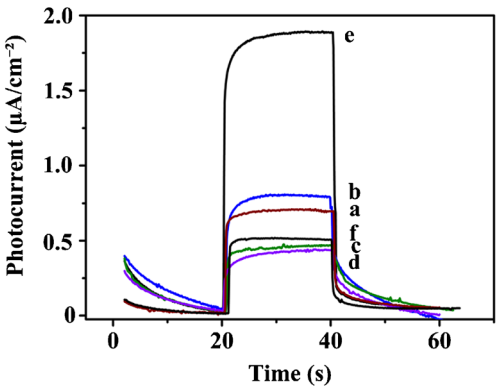


**Fig. 2** The PEC response of different electrodes in 0.1 M phosphate buffer containing 0.1 M AA (pH 7.4). (**a**) g-$C_3N_4$/ITO, (b) g-$C_3N_4$-AuNP/ITO, (**c**) Peptide/g-$C_3N_4$-AuNP/ITO, (**d**) P-Peptide/g-$C_3N_4$-AuNP/ITO, (**e**) CdS/P-Peptide/g-$C_3N_4$-AuNP/ITO, (**f**) Peptide/g-$C_3N_4$-AuNP/ITO after incubated with CdS QDs

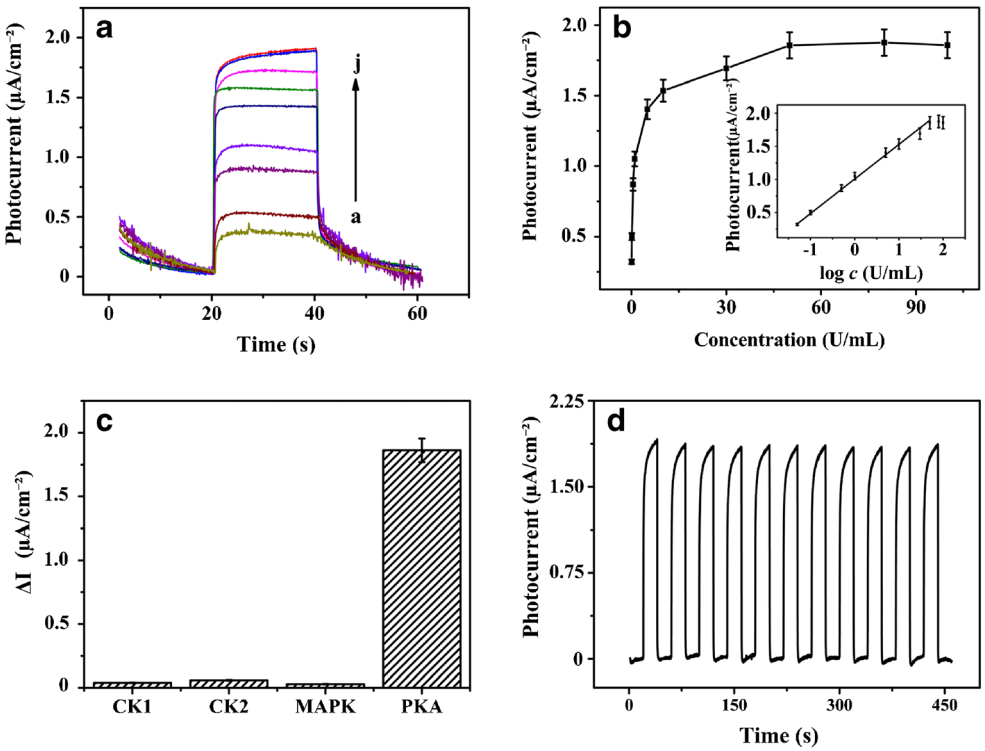


**Fig. 3** (**a**) The PEC response of CdS/P-Peptide/g-$C_3N_4$-AuNP/ITO electrode with different PKA concentrations. a − j, 0.05, 0.1, 0.5, 1, 5, 10, 30, 50, 80, 100 U/mL. (**b**) The relationship between PKA concentration and the photocurrent density. The insert graph is the linear relationship between the PEC intensity and the logarithm value of PKA concentrations. (**c**) PEC intensity change after Peptide/g-$C_3N_4$-AuNP/ITO was incubated successively with 50 U/mL different kinases and 40 μL of CdS QDs. (**d**) PEC response of CdS/P-Peptide/g-$C_3N_4$-AuNP/ITO in detection buffer for 11 times

the electrostatic repulsion effect. Whereas, after the capture of CdS QDs on P-Peptide/g-$C_3N_4$-AuNP/ITO electrode surface, the photocurrent density increases significantly (curve e). Under illumination, the electrons would quickly jump from the conduction band of CdS QDs to the conduction band of g-$C_3N_4$, while the holes of g-$C_3N_4$ would migrate to the surface of CdS QDs. The presence of CdS QDs accelerate the spatial charge separation, thus preventing the electron–hole recombination, thereby increasing the photocurrent response.

To further confirm the crucial effect of phosphorylation on the capture of CdS QDs, another control experiment was performed. To perform it, Peptide/g-$C_3N_4$-AuNP/ITO electrode was directly incubated with CdS QDs, and then the photocurrent was recorded in detection buffer. As seen in Fig. 2, curve f, the photocurrent density of this electrode is much weaker than that obtained at CdS/P-Peptide/g-$C_3N_4$-AuNP/ITO (curve e). Based on the above researches, we believe that this PEC method can be applied for PKA activity detection.

**Table 1** Comparison of detection performances of this PEC method with other methods for protein kinase detection

| Methods | Linear range (unit/mL) | LOD (unit/mL) | Refs. |
|---|---|---|---|
| Electrochemiluminescence | 0.05–5 | 0.04 | [23] |
| Electrochemiluminescence | 0.01–20 | 0.005 | [24] |
| Fluorescence | 1–2000 | 0.5 | [25] |
| Fluorescence | 0.001–0.05 | 0.0005 | [26] |
| Fluorescence | 0.05–1.6 | 0.02 | [27] |
| Electrochemistry | 0.05–100 | 0.014 | [8] |
| Electrochemistry | 0.1–50 | 0.026 | [28] |
| Electrochemistry | 0.1–1 | 0.09 | [29] |
| Electrochemistry | 0.005–500 | 0.002 | [30] |
| Electrochemistry | 2–50 | 0.05 | [31] |
| Colorimetry | 0.5–50 | 0.5 | [32] |
| Colorimetry | 0.1–0.5 | 0.0375 | [33] |
| Photoelectrochemistry | 0.1–100 | 0.048 | [5] |
| Photoelectrochemistry | 0.05–50 | 0.077 | [34] |
| Photoelectrochemistry | 0.05–50 | 0.017 | This work |

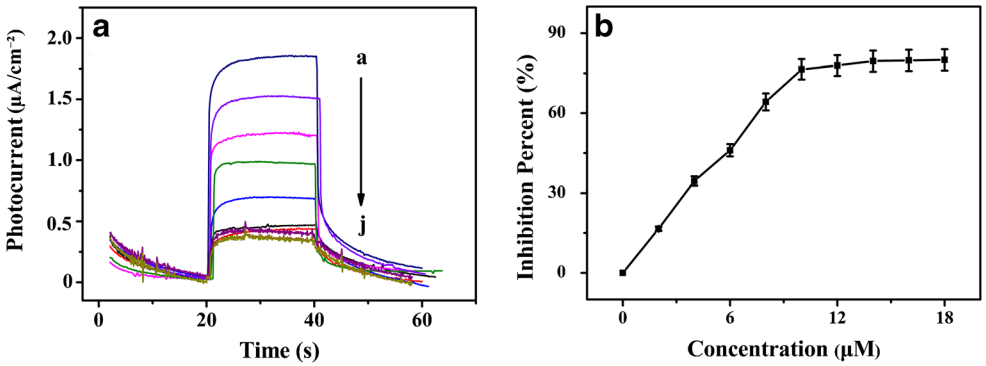


**Fig. 4** (**a**) PEC response of the CdS/P-Peptide/g-$C_3N_4$-AuNP/ITO, which was fabricated with different concentrations of ellagic acid in 100 mM Tris-HCl and 100 mM AA (pH 7.4). a − j, 0, 2, 4, 6, 8, 10, 12, 14, 16 and 18 μM. PKA concentration is 50 U/mL. Applied potential, −0.3 V. Irradiation, Visible Light. (**b**) The plot for the relationship between ellagic acid concentration and inhibition percent

## Optimization of experimental conditions

The following parameters were optimized: (a) g-$C_3N_4$-AuNPs concentration; (b) PKA catalysis time; (c) CdS QDs reaction time. Respective data and Figures are given in the Supporting Information. The following experimental conditions were found to give best results: (a) g-$C_3N_4$-AuNPs concentration of 2.0 mg/mL; (b) PKA catalysis time of 40 min; (c) CdS QDs reaction time of 12 h.

## Analytical performance

Under optimum conditions, the relationship between PKA concentration and the photocurrent density of the electrode was investigated. As can be seen in Fig. 3a and b, the photocurrent density enhances gradually with increasing the PKA concentration from 0.05 to 50 unit/mL. When PKA concentration is higher than 50 unit/mL, the photocurrent density tends to level off. The photocurrent density is proportional to the logarithm value of PKA concentration in the range of 0.05–50 unit/mL with the linear regression equation of $I$ (nA) = 104.3lg$c$ (unit/mL) + 201.5 ($R$ = 0.9907). The detection limit is estimated to be 0.017 unit/mL (S/$N$ = 3). The detection performance of this method was compared with some previous reports. From Table 1, we can get a report that the detection limit of our work is lower and the linear range of our work is wider than some of previous reports. Comprehensive consideration of the inherent advantage of our method, such as miniaturization of the instrument, low sample consumption, fast detection speed, good specificity, high sensitivity, our method might be an ideal platform for protein kinase activity assay.

As a potentially applicable analysis method, it should have not only low detection limit and wide linear range, but also excellent detection specificity and reproducibility. Thus, these properties were investigated. To investigate the specificity of this method, three protein kinases (MAPK, CK1, CK2) were selected as comparative reagents. The photocurrent density change ($\Delta I = I_1$-$I_2$) of CdS/P-Peptide/g-$C_3N_4$-AuNP/ITO prepared with different protein kinases were compared, where $I_1$ is the photocurrent density of CdS/P-Peptide/g-$C_3N_4$-AuNP/ITO fabricate with 50 U/mL of different protein kinases, $I_2$ is the photocurrent density of CdS/P-Peptide/g-$C_3N_4$-AuNP/ITO fabricated with 0 U/mL PKA). As shown in Fig. 3c, the $\Delta I$ for MAPK, CK1 and CK2 is significantly lower than that for PKA, indicating that this method had good specificity. The

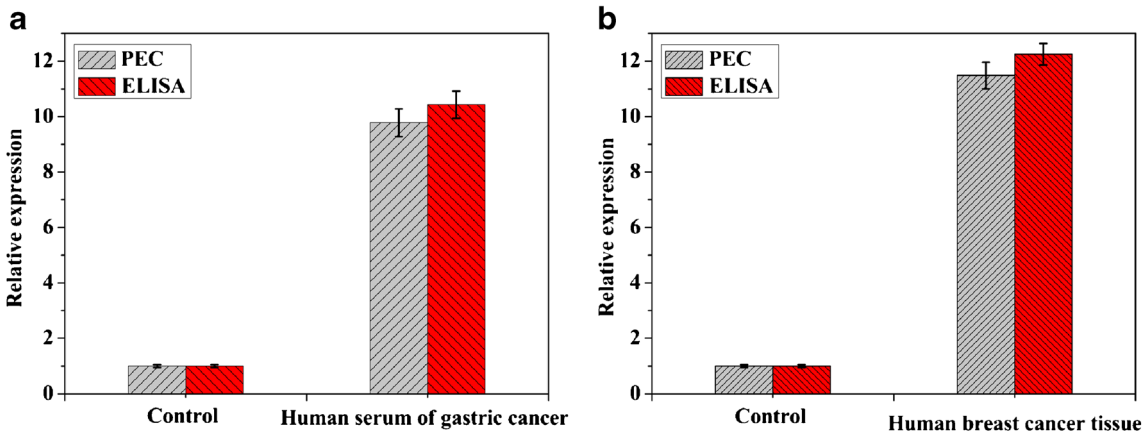


**Fig. 5** The histogram of the relative activity of PKA in different samples

reproducibility of the PEC method was investigated by comparing the photocurrent density of ten CdS/P-Peptide/g-$C_3N_4$-AuNP/ITO electrodes, where these electrodes were prepared with the same procedure as described in section of Electrode fabrication. As illustrated in Fig. S2, there are no significant difference among the photocurrent density of ten independent electrodes. The relative standard deviation (RSD) for ten determinations is 1.30%, indicating that the experimental strategy showed good reproducibility.

The stability is another crucial factor for the PEC method, and it was evaluated by detecting the photocurrent density of CdS/P-peptide/g-$C_3N_4$-AuNP/ITO in detection buffer. As show in Fig. 3d, there is no significant change of photocurrent response observed with light on and off continuing 460 s for 11 times. And the relative standard deviation (RSD) is 1.65%. In addition, this method was constructed by PKA catalysis. Because PKA is easy to be inactive, it's better to do the detection once the electrode is prepared. It retains 94% of the initial response for after one week in the refrigerator at 4 °C. Therefore, those results indicated the method has good stability.

### Inhibition investigation

The screening of small molecule inhibitors for protein kinase was of high importance in the discovery of kinase-targeted anticancer pharmaceuticals. In order to prove the potential application of our experimental strategy in the screening of protein kinase inhibitors, we conducted an experimental study using inhibitor of ellagic acid. As shown in Fig. 4, as the concentration of ellagic acid increases, the photocurrent density decreases gradually, indicating that ellagic acid can inhibit PKA activity and then block the phosphorylation event. When the concentration of ellagic acid is greater than 10 μM, the percentage of inhibition almost no longer changes. The figure shows that the $IC_{50}$ (The half maximal inhibitory concentration) is about 6.5 μM, which is comparable with some previous results, such as which is comparable with some previous results, such as 4.22 μM [23], 3.57 μM [24], 3.98 μM [25], 2.77 μM [26], 9.10 μM [27] and 2.10 μM [5]. The results show that the experimental strategy investigated in this experiment has a potential application in the screening of protein kinase inhibitors.

### Detection of PKA activity in real samples

In order to study the applicability of the PEC method for PKA activity detection in real samples, we examined PKA activity in the serum of breast cancer patients and breast tissue of breast cancer patients. In contrast, the PKA activity in serum and breast tissue of healthy people were detected as control. As shown in Fig. 5, the PKA activity in the patients is higher than that in healthy individuals. To further prove the detection validity, the activity of PKA was also determined by PKA kinase activity assay kit, and the results are comparable with that obtained by our method, indicating that our method also shows high detection accuracy.

The results showed that this method has potential application value in the early diagnosis of cancer.

## Conclusion

In summary, a sensitive and selective PEC method is investigated for PKA activity assay and inhibitor screening, in which g-$C_3N_4$ is used as photoactive material, CdS QDs as signal amplification unit. This PEC method presents several distinct advantages. Firstly, the photoactive material of g-$C_3N_4$ is metal-free, which is friendlier to environment than metal-contained photoactive material. Moreover, the easy preparation of g-$C_3N_4$ also facilitates the electrode fabrication. Then, the photoactivity of g-$C_3N_4$ is greatly improved through the introducing of CdS QDs. According to these advantages, the high sensitive and selective assay of protein kinase activity and inhibitor screening are testified. However, the limitation of this detection strategy is a little time-consuming. If we can decrease the fabrication time, our strategy will be a fine and rapid method for protein kinase A detection. Even so, the method is also successfully applied to detect protein kinase activity in cell lysates, which illustrates the great potential for kinase-related drug discovery, early diagnosis of disease and evaluation of therapeutic efficacy.

**Acknowledgements** This work was supported by the National Natural Science Foundation of China (No. 21775090, 21375079), the Natural Science Foundation of Shandong province, China (No. ZR2014BQ029).

**Compliance with ethical standards** The author(s) declare that they have no competing interests.

## References

1. Del Gobbo A, Peverelli E, Treppiedi D, Lania A, Mantovani G, Ferrero S (2016) Expression of protein kinase a regulatory subunits in benign and malignant human thyroid tissues: a systematic review. Exp Cell Res 346(1):85–90. https://doi.org/10.1016/j.yexcr.2016.06.004
2. Augustinack JC, Schneider A, Mandelkow E-M, Hyman BT (2001) Specific tau phosphorylation sites correlate with severity of neuronal cytopathology in Alzheimer's disease. Acta Neuropathol 103(1):26–35. https://doi.org/10.1007/s004010100423
3. Huamin Wang AD, Yu S, Ahmed K (2001) Response of cancer cells to molecular interruption of the CK2 signal. Mol Cell Biochem 227(1–2):167–174. https://doi.org/10.1023/A:1013112908734
4. Forst T, Weber MM, Pfutzner A (2012) Cardiovascular benefits of GLP-1-based herapies in patients with diabetes mellitus type 2: effects on endothelial and vascular dysfunction beyond glycemic control. Exp Diabetes Res 2012(635472):1–9. https://doi.org/10.1155/2012/635472
5. Li X, Zhu L, Zhou Y, Yin H, Ai S (2017) Enhanced photoelectrochemical method for sensitive detection of protein

kinase a activity using $TiO_2$/g-$C_3N_4$, PAMAM dendrimer, and alkaline phosphatase. Anal Chem 89(4):2369–2376. https://doi.org/10.1021/acs.analchem.6b04184
6. Kerman K, Kraatz H-B (2009) Electrochemical detection of protein tyrosine kinase-catalysed phosphorylation using gold nanoparticles. Biosens Bioelectron 24(5):1484–1489. https://doi.org/10.1016/j.bios.2008.10.024
7. Liu X, Li Y, Xu X, Li P, Nie Z, Huang Y, Yao S (2014) Nanomaterial-based tools for protein kinase bioanalysis. Tractrend Anal Chem 58:40–53. https://doi.org/10.1016/j.trac.2014.01.009
8. Zhou Y, Yin H, Li X, Li Z, Ai S, Lin H (2016) Electrochemical biosensor for protein kinase a activity assay based on gold nanoparticles-carbon nanospheres, phos-tag-biotin and beta-galactosidase. Biosens Bioelectron 86:508–515. https://doi.org/10.1016/j.bios.2016.07.004
9. Zhao WW, Xu JJ, Chen HY (2014) Photoelectrochemical DNA biosensors. Chem Rev 114(15):7421–7441. https://doi.org/10.1021/cr500100j
10. Cheng W, Pan J, Yang J, Zheng Z, Lu F, Chen Y, Gao W (2018) A photoelectrochemical aptasensor for thrombin based on the use of carbon quantum dot-sensitized $TiO_2$ and visible-light photoelectrochemical activity. Microchim Acta 185(5):263. https://doi.org/10.1007/s00604-018-2800-z
11. Zhang B, Lu L, Hu Q, Huang F, Lin Z (2014) ZnO nanoflower-based photoelectrochemical DNAzyme sensor for the detection of $Pb^{2+}$. Biosens Bioelectron 56:243–249. https://doi.org/10.1016/j.bios.2014.01.026
12. Wu S, Huang H, Shang M, Du C, Wu Y, Song W (2017) High visible light sensitive $MoS_2$ ultrathin nanosheets for photoelectrochemical biosensing. Biosens Bioelectron 92:646–653. https://doi.org/10.1016/j.bios.2016.10.037
13. Wang M, Yin H, Shen N, Xu Z, Sun B, Ai S (2014) Signal-on photoelectrochemical biosensor for microRNA detection based on $Bi_2S_3$ nanorods and enzymatic amplification. Biosens Bioelectron 53:232–237. https://doi.org/10.1016/j.bios.2013.09.069
14. Zhou Y, Xu Z, Wang M, Sun B, Yin H, Ai S (2014) DNA methyltransferase activity assay based on visible light-activated photoelectrochemical biosensor. Biosens Bioelectron 53:263–267. https://doi.org/10.1016/j.bios.2013.09.065
15. Li B, Yin H, Zhou Y, Wang M, Wang J, Ai S (2018) Photoelectrochemical detection of miRNA-319a in rice leaf responding to phytohormones treatment based on CuO-$CuWO_4$ and rolling circle amplification. Sensors Actuators B Chem 255:1744–1752. https://doi.org/10.1016/j.snb.2017.08.192
16. Wang H, Yin H, Huang H, Li K, Zhou Y, Waterhouse GIN, Lin H, Ai S (2018) Dual-signal amplified photoelectrochemical biosensor for detection of N(6)-methyladenosine based on $BiVO_4$-110-$TiO_2$ heterojunction, $ag^{(+)}$-mediated cytosine pairs. Biosens Bioelectron 108:89–96. https://doi.org/10.1016/j.bios.2018.02.056
17. Dai L, Du X, Jiang D, Chen W, Zhu M, Wang K (2016) Ultrafine α-$Fe_2O_3$ nanocrystals anchored on N-doped graphene: a nanomaterial with long hole diffusion length and efficient visible light-excited charge separation for use in photoelectrochemical sensing. Microchim Acta 184(1):137–145. https://doi.org/10.1007/s00604-016-1989-y
18. Ong W-J, Tan L-L, Ng YH, Yong S-T, Chai S-P (2016) Graphitic carbon nitride (g-$C_3N_4$)-based photocatalysts for artificial photosynthesis and environmental remediation: are we a step closer to achieving sustainability? Chem Rev 116(12):7159–7329. https://doi.org/10.1021/acs.chemrev.6b00075
19. Xi X, Li J, Wang H, Zhao Q, Li H (2015) Non-enzymatic photoelectrochemical sensing of hydrogen peroxide using hierarchically structured zinc oxide hybridized with graphite-like carbon nitride. Microchim Acta 182(7–8):1273–1279. https://doi.org/10.1007/s00604-015-1448-1
20. Han KK, Wang CC, Li YY, Wan MM, Wang Y, Zhu JH (2013) Facile template-free synthesis of porous g-$C_3N_4$ with high photocatalytic performance under visible light. RSC Adv 3(24):9465. https://doi.org/10.1039/c3ra40765a
21. Chen L, Zeng X, Si P, Chen Y, Chi Y, Kim DH, Chen G (2014) Gold nanoparticle-graphite-like $C_3N_4$ nanosheet nanohybrids used for electrochemiluminescent immunosensor. Anal Chem 86(9):4188–4195. https://doi.org/10.1021/ac403635f
22. Li R, Liu Y, Yan T, Li Y, Cao W, Wei Q, Du B (2015) A competitive photoelectrochemical assay for estradiol based on in situ generated CdS-enhanced $TiO_2$. Biosens Bioelectron 66:596–602. https://doi.org/10.1016/j.bios.2014.12.002
23. Liu J, He X, Wang K, He D, Wang Y, Mao Y, Shi H, Wen L (2015) A highly sensitive electrochemiluminescence assay for protein kinase based on double-quenching of graphene quantum dots by G-quadruplex-hemin and gold nanoparticles. Biosens Bioelectron 70:54–60. https://doi.org/10.1016/j.bios.2015.03.026
24. Zhang G-Y, Cai C, Cosnier S, Zeng H-B, Zhang X-J, Shan D (2016) Zirconium–metalloporphyrin frameworks as a three-in-one platform possessing oxygen nanocage, electron media, and bonding site for electrochemiluminescence protein kinase activity assay. Nanoscale 8(22):11649–11657. https://doi.org/10.1039/c6nr01206j
25. Shen C, Xia X, Hu S, Yang M, Wang J (2015) Silver nanoclusters-based fluorescence assay of protein kinase activity and inhibition. Anal Chem 87(1):693–698. https://doi.org/10.1021/ac503492k
26. Zhang K, Zeng K, Shen C, Tian S, Yang M (2018) Determination of protein kinase a activity and inhibition by using hydroxyapatite nanoparticles as a fluorescent probe. Microchim Acta 185(4):225. https://doi.org/10.1007/s00604-018-2754-1
27. Liu Q, Na W, Wang L, Su X (2017) Gold nanocluster-based fluorescent assay for label-free detection of protein kinase and its inhibitors. Microchim Acta 184(9):3381–3387. https://doi.org/10.1007/s00604-017-2349-2
28. Zhou Y, Wang M, Yin H, Ai S (2017) Amperometric determination of the activity of protein kinase a using a glassy carbon electrode modified with IgG functionalized gold nanoparticles conjugated to horseradish peroxidase. Microchim Acta 184(9):3301–3308. https://doi.org/10.1007/s00604-017-2341-x
29. Liu J, He X, Wang K, Wang Y, Yan G, Mao Y (2014) Amplified electrochemical detection of protein kinase activity based on gold nanoparticles/multi-walled carbon nanotubes nanohybrids. Talanta 129:328–335. https://doi.org/10.1016/j.talanta.2014.05.043
30. Shen C, Li X, Rasooly A, Guo L, Zhang K, Yang M (2016) A single electrochemical biosensor for detecting the activity and inhibition of both protein kinase and alkaline phosphatase based on phosphate ions induced deposition of redox precipitates. Biosens Bioelectron 85:220–225. https://doi.org/10.1016/j.bios.2016.05.025
31. Chand R, Han D, Shin IS, Hong JI, Kim YS (2015) Gold nanoparticle enhanced electrochemical assay for protein kinase activity using a synthetic chemosensor on a microchip. J Electrochem Soc 162(4):B89–B93. https://doi.org/10.1149/2.0821504jes
32. Sun S, Shen H, Liu C, Li Z (2015) Phosphorylation-regulated crosslinking of gold nanoparticles: a new strategy for colorimetric detection of protein kinase activity. Analyst 140(16):5685–5691. https://doi.org/10.1039/c5an00963d
33. Shen C, Zhang K, Gao N, Wei S, Liu G, Chai Y, Yang M (2016) Colorimetric and electrochemical determination of the activity of protein kinase based on retarded particle growth due to binding of phosphorylated peptides to DNA - capped silver nanoclusters. Microchim Acta 183(11):2933–2939. https://doi.org/10.1007/s00604-016-1944-y
34. Li X, Zhou Y, Xu Y, Xu H, Wang M, Yin H, Ai S (2016) A novel photoelectrochemical biosensor for protein kinase activity assay based on phosphorylated graphite-like carbon nitride. Anal Chim Acta 934:36–43. https://doi.org/10.1016/j.aca.2016.06.024